The Journal of Eukaryotic Microbiology

ISOP Published by the International Society of Protistologists

Journal of Eukaryotic Microbiology ISSN 1066-5234

ORIGINAL ARTICLE

Ultrastructural Comparison of *Hepatozoon ixoxo* and *Hepatozoon theileri* (Adeleorina: Hepatozoidae), Parasitising South African Anurans

Roxanne Conradie[a], Courtney A. Cook[a], Louis H. du Preez[a,b], Anine Jordaan[c] & Edward C. Netherlands[a,d]

a Unit for Environmental Sciences and Management, North-West University, Potchefstroom 2520, South Africa
b South African Institute for Aquatic Biodiversity, Private Bag 1015, Grahamstown 6140, South Africa
c Laboratory for Electron Microscopy, Chemical Resource Beneficiation, North-West University, Potchefstroom 2520, South Africa
d Laboratory of Aquatic Ecology, Evolution and Conservation, University of Leuven, Leuven 3000, Belgium

Keywords
Anura; apicomplexan; blood parasite; haemogregarine; haemoparasite. morphology; SEM; TEM; ultrastructure.

Correspondence
E.C. Netherlands, Unit for Environmental Sciences and Management, Potchefstroom Campus, North-West University, Private Bag X6001, Potchefstroom 2520, South Africa
Telephone number: +27(0)18-299-2515;
FAX number: +27(0)18-299-2503;
e-mail: ec.netherlands@gmail.com

Received: 8 April 2016; revised 11 July 2016; accepted July 25, 2016.
Early View publication August 23, 2016

doi:10.1111/jeu.12351

ABSTRACT

To date, only two haemogregarine parasite species have been described from South African anurans: *Hepatozoon ixoxo*, infecting toads of the genus *Sclerophrys* (syn. *Amietophrynus*); and *Hepatozoon theileri*, parasitising the common river frog, *Amietia quecketti*. Both species have been characterised using limited morphology, and molecular data from PCR amplified fragments of the 18S rRNA gene. However, no ultrastructural work has been performed thus far. The aim of this study was to add descriptive information on the two species by studying their ultrastructural morphology. Mature gamont stages, common in the peripheral blood of infected frogs, were examined by transmission electron microscopy. Results indicate that *H. ixoxo* and *H. theileri* share typical apicomplexan characteristics, but differ markedly in their external cellular structure. *Hepatozoon ixoxo* is an encapsulated parasite presenting a prominent cap at the truncate pole, and shows no visible modifications to the host cell membrane. In comparison, *H. theileri* does not present a capsule or cap, and produces marked morphological changes to its host cell. Scanning electron microscopy was performed to further examine the cytopathological effects of *H. theileri*, and results revealed small, knob-like protrusions on the erythrocyte surface, as well as notable distortion of the overall shape of the host cell.

HAEMOGREGARINES of the genus *Hepatozoon* Miller, 1908 are apicomplexan blood parasites with complex life cycles involving a vertebrate host and an arthropod vector (Smith 1996). More than 300 *Hepatozoon* species have been described from vertebrates with at least 40 species recorded infecting anurans (Smith 1996). Over the last century of research on intraerythrocytic parasites, there has been a greater focus on those that are of veterinary or medical importance (Davies and Johnston 2000), such as haemogregarines causing canine hepatozoonosis (Boulianne et al. 2007). Conversely, literature regarding the blood parasites of ectothermic wildlife is sparser, especially with regard to amphibians (Davies and Johnston 2000). Only two anuran *Hepatozoon* species have currently been recorded from South Africa, *Hepatozoon theileri* (Laveran, 1905) and *Hepatozoon ixoxo* Netherlands, Cook and Smit, 2014. In the light of South Africa's rich frog biodiversity, this limited account may indicate a lack of knowledge regarding the country's amphibian blood parasites.

Hepatozoon ixoxo is a generalist, parasitising at least three frog species of the Bufonidae: *Sclerophrys garmani* (Meek, 1897), *Sclerophrys gutturalis* (Meek, 1897), and *Sclerophrys maculatus* (Meek, 1897) (type host) (see Netherlands et al. 2014a). This species also possibly infects several other frog species from the Hemisotidae, Phrynobatrachidae, and Ptychadenidae (see Netherlands et al. 2015). On the other hand, *H. theileri* appears to be host-specific to the common river frog, *Amietia quecketti* (Boulenger, 1895) (type host), Pyxicephalidae (Netherlands et al. 2014b). *Hepatozoon ixoxo* has been described only recently, supplementing the morphological description with molecular data (Netherlands et al. 2014a), as compared to *H. theileri*. The latter was originally classified as a member of the genus *Haemogregarina* Danilewsky, 1885

by Laveran in 1905, but based on morphology and life cycle dynamics, Smith (1996) transferred it to the genus *Hepatozoon*. This taxonomic reclassification was recently confirmed in a morphometric and molecular redescription, using a fragment of the 18S rRNA gene (Netherlands et al. 2014b).

Apicomplexan parasites are classified according to genetic comparisons, life-cycle descriptions, and developmental patterns in vertebrate and invertebrate hosts (Smith et al. 1999). The ultrastructure of parasite stages provides a diagnostic tool in the characterisation process (Siddall and Desser 1992) and adds reliability to taxonomic descriptions (Smith and Desser 1997). As intraerythrocytic gamonts are frequently found in peripheral blood, this developmental stage was used for comparison. The aim of this study was to provide additional knowledge on the morphology of the currently known frog haemogregarines known from South Africa. This is the first report on the ultrastructure of apicomplexan frog haemoparasites in Africa.

MATERIALS AND METHODS

Collection and maintenance of experimental animals

Flat-backed toads (*S. maculatus*) were collected by hand at night from Ndumo Game Reserve, Kwa-Zulu Natal, from a riverine site (27°23′26″S, 32°08′24″E), in April 2013, forming part of a previous study on *H. ixoxo* (see Netherlands et al. 2014a). Similarly, common river frogs (*A. quecketti*) were collected from artificial ponds at the North-West University Botanical Gardens, Potchefstroom (26°40′56″S, 27°05′43″E), in March 2015. This population was chosen as these frogs have been identified in past studies (Netherlands et al. 2014b) to harbour *H. theileri*. For both sampling efforts, thin blood smears were prepared and screened following the methods of Netherlands et al. (2014a). Parasitaemia was calculated per 100 erythrocytes, with 5,000 erythrocytes examined per blood smear, and expressed as a percentage.

All frogs were released at the site of capture, with the exception of the two *S. maculatus* from the previous study (see Netherlands et al. 2014a), and one *A. quecketti* from the Botanical Gardens. These individual frogs were selected for monitoring purposes, due to their high parasitaemia values. They were kept in separate vivaria and maintained on a diet of gut loaded common garden crickets (*Gryllus bimaculatus*). The *S. maculatus* specimens were monitored for parasite stages and parasitaemia levels on a bimonthly basis (see Netherlands et al. 2014a), and the *A. quecketti* every third month. This was done to allow specimens to recover from continuous blood extractions and prevent anaemia.

DNA extraction and phylogenetic analysis

To confirm that the mature gamonts found in the two frog species were indeed *H. ixoxo* and *H. theileri*, genetic analysis was performed to ensure accuracy, following Netherlands et al. (2014a).

Based on molecular evidence, 18S rDNA sequences were identified as *H. ixoxo* and *H. theileri* using the Basic Local Alignment Search Tool (BLAST) (http://www.ncbi.nlm.nih.gov/blast). Uncorrected pair-wise distances (p-distance) and base pair differences were determined with the MEGA6 bioinformatics software program (http://www.megasoftware.net). The aligned sequences between all available sequences of *H. ixoxo* [Genbank: KP119770; KP119771; KP119772] and *H. theileri* [GenBank: KP119773; KJ599676] were compared to the sequences obtained in this study. The analysis involved seven nucleotide sequences. All positions with less than 95% site coverage were eliminated. That is, fewer than 5% alignment gaps, missing data, and ambiguous bases were allowed at any position. Sequences were deposited in the NCBI GenBank database under the accession numbers: KX512803–KX512804.

Transmission electron microscopy (TEM)

Samples were prepared for ultrastructural analysis using peripheral blood drawn from a *S. maculatus* specimen with a 9.2% parasitaemia, and the *A. quecketti* specimen with a parasitaemia level of 7.7%. Approximately, three drops of blood were immediately prefixed for 12 h in 0.5 ml Todd's fixative (Todd 1986) at 4°C. The sample was then washed three times for 15 min each in 0.05 M cacodylate buffer (pH 7.4). Osmium tetroxide (1% W/V) in the same buffer was used to postfixate the sample for one hour. The sample was thereafter washed three times in cacodylate buffer, followed by dehydration of the sample in an ascending graded ethanol series (50%, 70%, 90%, and 100% × 2 for 15 min each). Care was taken during this process to ensure that the sample did not come into contact with air. The 100% ethanol was then replaced with 100% LR White™ resin for 15 min and placed in a rotator to ensure optimal penetration of the resin and to prevent premature polymerisation of the sample. This was then replaced with fresh resin twice, rotated for 45 min each time, and then left overnight in a refrigerator at 4°C. Samples were then embedded in fresh resin and placed in gelatine capsules. This was followed by oven-curing at 65°C for 12 h.

Glass knives were used to cut approximately 90 nm ultrathin sections with a Reichert-Jung Ultracut Ultramicrotome™. Sections were positioned onto 3 mm copper grids, stained with 4% uranyl acetate for 2 min, and washed in dH_2O for 1 min. After the sample had dried, the samples were stained using Reynold's lead citrate for a few seconds, washed in dH_2O for 1 min, and left to dry. Specimens were examined with an FEI Tecnai G2 20-S Twin high resolution TEM at 120 kV, and micrographs digitally captured with a Gatan bottom mount camera and Digital Micrograph software.

Scanning electron microscopy (SEM) of *Hepatozoon theileri*

To gain a better understanding of the effect caused by *H. theileri* on the host erythrocytes, blood was collected

from the same *A. quecketti* specimen, as described above for TEM. This was not done for *H. ixoxo*, as no obvious effects were observed in the TEM sections of *H. ixoxo* on its host cell, i.e., dehaemoglobinisation, or the protruding nodules of the host erythrocyte. A thin smear of blood was prepared on a 10 mm circular glass coverslip, and a drop of Todd's fixative (Todd 1986) placed on the blood film before it dried. After waiting roughly a minute, the glass coverslip was submerged in fresh Todd's fixative and allowed to fixate for 2 h. The sample was then gently washed with ultrapure water three times each for 15 min. Postfixation was performed with 2% osmium tetroxide (OsO_4) for 90 min. This was followed by rinsing three times in ultrapure water for 10 min, followed by dehydration in an ethanol series (30%, 50%, 70%, 80%, 96%, and twice in absolute alcohol, each for 10 min). The material was then critical point dried using liquid carbon dioxide. The glass coverslips were placed into histology cassettes, and the cassettes placed into the chamber of the critical point dryer (Bio-Rad, Bio-Rad Microscience Division, United Kingdom). The coverslips were mounted onto 12 mm aluminium stubs with double-sided carbon tape and sputter-coated for 2 min with a gold palladium alloy, in argon gas at a pressure of 2 atm (SPI-Module™ Sputter Coater, SPI Supplies, West Chester, PA, USA). Specimen stubs were stored in a desiccator for at least 1 h before being examined by SEM at an accelerated voltage of 10 kV (Phenom PRO Desktop SEM, Phenom-World B., Eindhoven, Netherlands).

RESULTS

General observations

BLAST results from the 18S rDNA sequence fragment (1,030 nt) obtained from both *S. maculatus* and *A. quecketti* in this study revealed a 100% identity to *H. ixoxo* [GenBank: KP119770; KP119771; KP119772] and *H. theileri* [GenBank: KP119773] on GenBank, respectively. In addition, the pairwise differences based on the base differences per site between these sequences confirmed that the haemogregarine species were indeed *H. ixoxo* [GenBank: KX512803] and *H. theileri* [GenBank: KX512804] (see Table 1), and further analysis could be continued.

The most frequently encountered stages within erythrocytes were mature gamont stages, with immature gamonts found occasionally for both species at different times of the monitored period. Trophozoite, meront, and merozoite stages had been found in the two *S. maculatus* specimens during a previous study, although they were rare (see Netherlands et al. 2014a). There was no observable sexual dimorphism in mature gamonts of either species, therefore, appearing to be isogamous. This is common in many other species of *Hepatozoon* and *Haemogregarina* (see Davies and Johnston 2000).

It was evident by light microscopy of Giemsa stained blood smears that mature gamonts of both *H. ixoxo* (see Fig. 1A) and *H. theileri* (Fig. 1B) cause hypertrophy of the host cell. However, notable differences in morphology were observable between these two species. A prominent pink-staining cap is present at the truncate pole of *H. ixoxo*, the parasite also encased by a well-defined wall, a type of thick capsule/parasitophorous vacuole (PV). These characteristics are absent in *H. theileri*, which had no cap and no thick-walled encasement, only a PV that appears as a cystic pocket on one side of the gamont. Displacement of the host nucleus was also different in both species, *H. ixoxo* causing displacement most often to one side of the gamont, whereas *H. theileri* frequently caused displacement to the anterior pole, opposite from the recurved tail. The overall shape of the infected erythrocytes, as well as their intracellular gamonts, also differed between species. Infected erythrocytes of *H. ixoxo* were generally rounder than the more elliptical *H. theileri*. A large portion of the *H. ixoxo* gamont appeared to be completely recurved so as to appear folded over on itself, whereas folding is not as notable in *H. theileri*. The recurved portion seen in the *H. ixoxo* gamont is approximately only a third to a quarter of the parasite length and has the appearance of a bent "tail". Retraction of the host cell haemoglobin was rare in *H. ixoxo* but was common in erythrocytes infected by *H. theileri*. Furthermore, intraerythrocytic *H. theileri* gamonts were sometimes found to have caused complete destruction of the host cell nucleus resulting in its complete absence (Fig. 1C). For more detail on the gamont morphology of *H. ixoxo* and *H. theileri* by light microscopy see (Netherlands et al. 2014a,b), respectively.

TEM of *Hepatozoon ixoxo* from *Sclerophrys maculatus*

Transmission electron microscopy revealed the presence of characteristic apicomplexan organelles, including rhoptries,

Table 1. Matrix showing ranges for uncorrected p-distances and ranges for base pair differences per site between sequences (below diagonal)

Species	1	2	3	4	5	6	7
1. KP119772 *Hepatozoon ixoxo* ex *Sclerophrys maculatus*		0.000	0.000	0.000	0.006	0.006	0.006
2. KP119770 *H. ixoxo* ex *Sclerophrys garmani*	0.000		0.000	0.000	0.006	0.006	0.006
3. KP119771 *H. ixoxo* ex *Sclerophrys gutturalis*	0.000	0.000		0.000	0.006	0.006	0.006
4. KX512803 *H. ixoxo* ex *S. maculatus*	0.000	0.000	0.000		0.006	0.006	0.006
5. KP119773 *Hepatozoon theileri* ex *Amietia quecketti*	0.017	0.017	0.017	0.017		0.000	0.000
6. KJ599676 *H. theileri* ex *A. quecketti*	0.017	0.017	0.017	0.017	0.000		0.000
7. KX512804 *H. theileri* ex *A. quecketti*	0.017	0.017	0.017	0.017	0.000	0.000	

Standard error estimate(s) are shown above the diagonal.

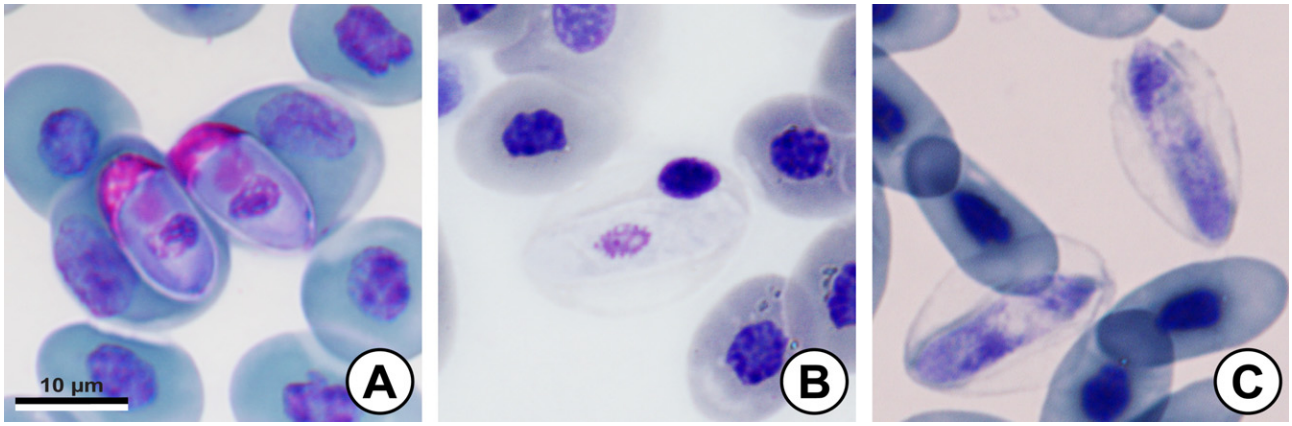

Figure 1 Light micrographs of *Hepatozoon* spp. in the peripheral blood of their anuran hosts. (**A**) Mature gamonts of *Hepatozoon ixoxo* infecting erythrocytes of *Sclerophrys maculatus*. Polar cap at the truncate pole stains a prominent pink, with hypertrophy of the host cell. (**B**) Peripheral blood of *Amietia quecketti* infected by mature gamonts of *Hepatozoon theileri*. The host nucleus is displaced towards the apical pole. (**C**) *Hepatozoon theileri* residing in host cells that have lost their nuclei.

micronemes, a conoid, and an anterior polar ring complex (Fig. 2A) (see Siddall and Desser 1992). Micrographs showed that the parasite was folded over on itself with its recurved "tail" sometimes extending to the anterior pole (Fig. 2A), the folding region occurring at the truncate pole. Rhoptries were positioned at the apical end of the parasite, visible in Fig. 2B. These were electron-dense, slightly club-shaped, and elongated organelles. Rounded, electron dense micronemes were smaller and more numerous than rhoptries.

At the top of the gamont apex, the conoid is apparent, with two preconoidal rings situated anteriad to this structure (Fig. 2B). The polar ring complex, containing approximately 85 subpellicular microtubules, occurs between subpellicular microtubules and the pellicle membranes (Fig. 2B). Figure 2C shows a lateral view of the polar ring complex with the conoid projecting from two adjacent layers, making up the inner membrane complex. An outer plasmalemma surrounds the inner membrane complex, making up a trilaminar pellicle (visible in Fig. 2B). The gamont was also encased by a prominent, thick capsule (Fig. 2B, D, E), which was sufficiently permeable to allow for good fixation of the encapsulated gamont. This capsule was interrupted at several distinct sites (sutures), which are clearly visible in Fig. 2F. These structures are apparent at opposite poles of the capsule.

The encapsulated gamont lay within a parasitophorous vacuole, separating it from the host cell (Fig. 2G). The pink-staining polar cap/cavity, evident by light microscopy, was visible by TEM as a homogenous, electron-dense region at the anterior pole of the parasite (Fig. 2H); it was also surrounded by the thick capsule but contained by the pellicle of the gamont. In some images of mature gamonts, the cytoplasm of the host cell appeared slightly less electron-dense in comparison with neighbouring uninfected red blood cells, indicating slight haemoglobin retraction in parasitised erythrocytes.

TEM of *Hepatozoon theileri* from *Amietia quecketti*

Transmission electron micrographs show that *H. theileri* causes notable modification to the structure of its host cell (Fig. 3A). The outer erythrocyte membrane had numerous uneven knob-like projections, jutting outwards from the cell, that was apparent when compared with uninfected erythrocytes (see Fig. 3B). These were inconsistent in height and distance from each other in some instances (Fig. 3C) and uniform in others (see Fig. 3D). A few images show that these protrusions are electron-dense structures (see Fig. 3D–F). On other areas of the membrane surface, it appears as though parts of the upper membrane are sloughing off (Fig. 3A, E). Infected cells possessed two long extensions protruding from the erythrocyte on the lateral sides of the gamont and composed likely only the host cell membrane (Fig. 3A, D, E). These extensions were variable in length and sometimes were twice as long as the width of the parasite itself.

Gamonts of *H. theileri* possessed electron-dense secretory organelles (Fig. 3A). These were difficult to differentiate as rhoptries or micronemes, as the organelles were similar in size and shape. In some images, they appeared to occur in bundles (Fig. 3F) (see Ostrovska and Paperna 1990). A few micrographs revealed higher concentrations of these osmophilic organelles at the anterior end of the parasite. The cytoplasm appeared granular, possessing lipid-like material in places. A few membrane-bound vesicles, a loose endoplasmic reticulum, and mitochondria were also observed. A conoid structure was present at the anterior end of the parasite, with a preconoidal ring visible at the apex (Fig. 3C). The number of microtubules continuing from the conoid was not evident.

The entire shape of the recurved gamont appeared ellipsoid. Figure 3G shows a free gamont. This parasite had a narrowed middle portion, which otherwise was the folded region when restricted to an erythrocyte. The posterior and anterior apices were slightly paddle-shaped (Fig. 3G),

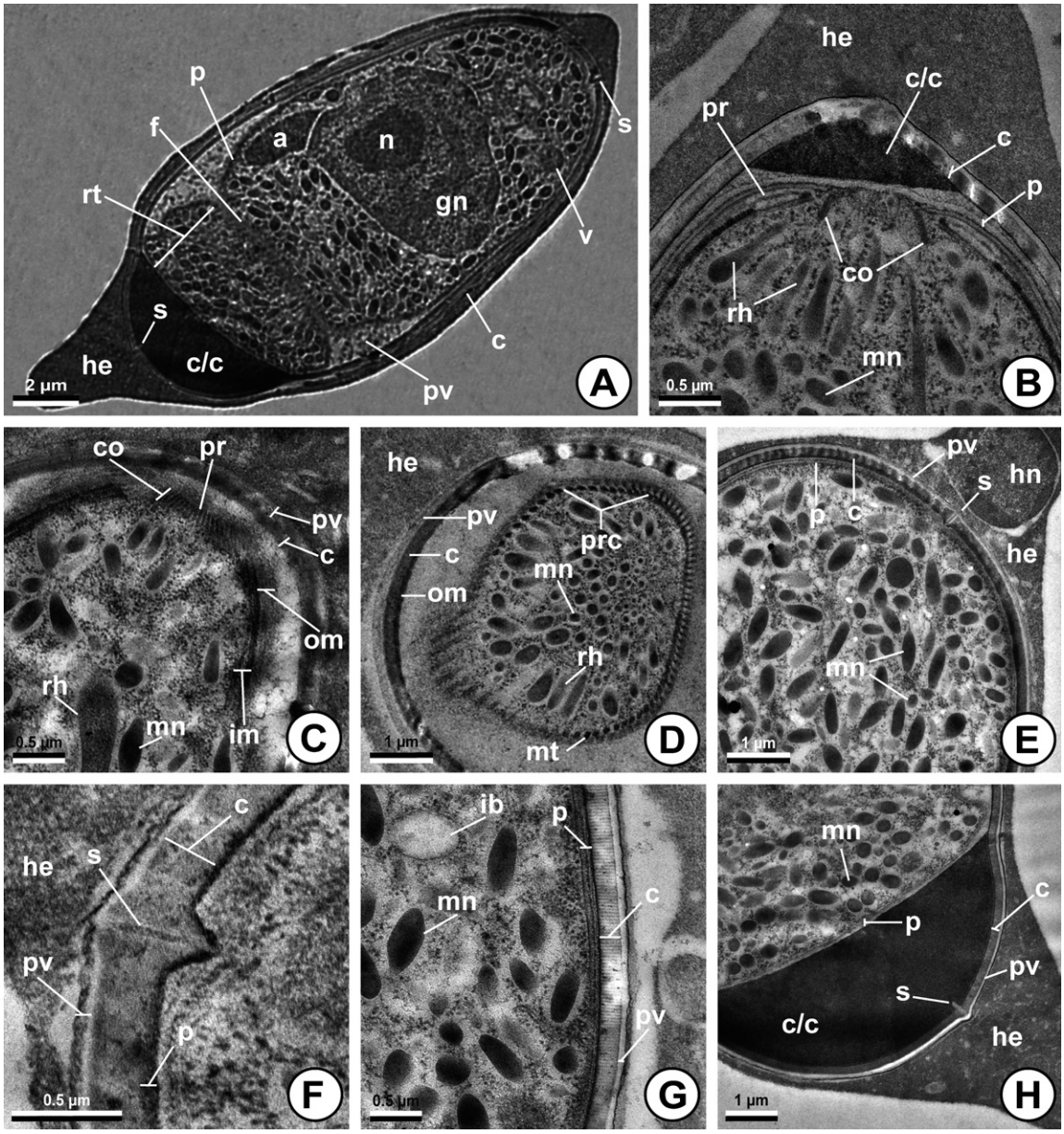

Figure 2 Transmission electron micrographs of *Hepatozoon ixoxo* in the peripheral blood of its anuran host, *Sclerophrys maculatus*. (**A**) Cross-section of a mature gamont lying within the host erythrocyte (he), with a recurved "tail" (rt), revealing the folding region (f). Gamont nucleus (gn) possesses an electrophilic nucleolus (n). Parasite surrounded by a trilaminar pellicle (p) and a parasitophorous vacuole (pv). Entire parasite and polar cap/cavity (c/c) encapsulated by a thick capsule (c), with sutures (s) at the apices. An apicoplast (a) and unknown vesicle (v) are present. (**B**) Micrograph showing a cross-section of the apical complex, with the conoid (co) lying within a polar ring (pr). Secretory organelles are present as rhoptries (rh) and micronemes (mn). A thick capsule (c), polar cap/cavity (c/c), host erythrocyte (he), and trilaminar pellicle (p) are visible. (**C**) Cross-section of the apical complex, showing the conoid (co), polar ring (pr), and areas of the outer membrane (om) and inner membrane (im) tapering together towards the conoid region. A thick capsule (c), micronemes (mn), parasitophorous vacuole (pv), and rhoptries (rh) are present. (**D**) Transverse section of the polar ring complex (prc) showing 85 microtubules (mt). The outer membrane (om) of the trilaminar pellicle is particularly evident as an electron dense layer. Other characters visible from the micrograph are the thick capsule (c), host erythrocyte (he), a few micronemes (mn), the parasitophorous vacuole (pv), and rhoptries (rh). (**E**) Host nucleus (hn) present with little dehaemoglobinisation evident in the host erythrocyte (he). Parasite surrounded by a thick capsule (c), pellicle (p), and parasitophorous vacuole (pv), with a suture (s) in the thick capsule near the host nucleus. Micronemes (mn) present. (**F**) Micrograph of the thick capsule (c), cleaved by a suture (s). A part of the host erythrocyte (he) is also visible, with dehaemoglobinisation not extensive. Also, present are the pellicle (p), and parasitophorous vacuole (pv). (**G**) Cross-section of the gamont wall, with a thick capsule (c) neighbouring the trilaminar pellicle (p). The capsule is encased by a parasitophorous vacuole (pv). A lipid body (lb) and micronemes (mn) are present. (**H**) A micrograph clearly showing the polar cap/cavity (c/c), containing electron dense material of unknown nature. Other features present are the thick capsule (c), host erythrocyte (he), pellicle (p), parasitophorous vacuole (pv), micronemes (mn), and a suture (s) visible at the apex within the thick capsule.

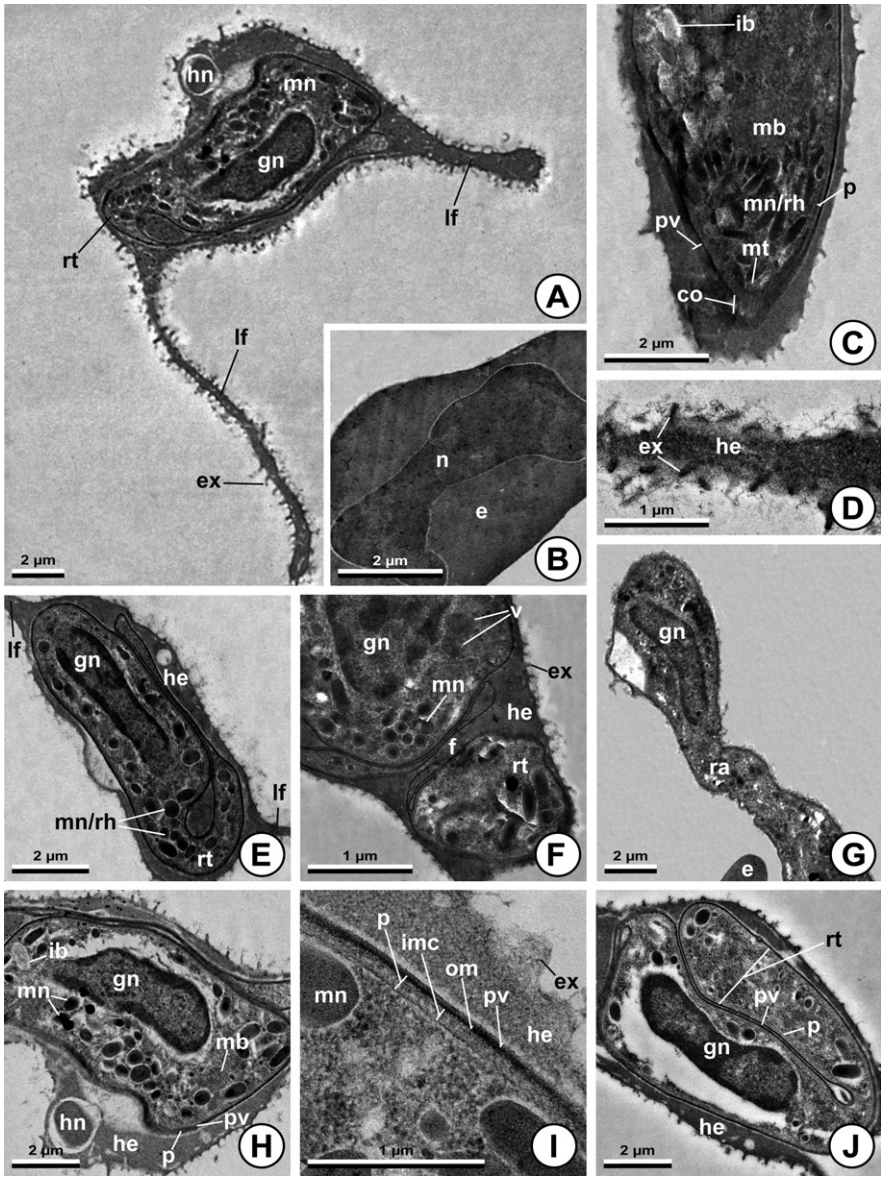

Figure 3 Transmission electron micrographs of *Hepatozoon theileri* in the peripheral blood of *Amietia quecketti*. (**A**) Mature gamont within a host erythrocyte. Excrescences or protrusions (ex) are visible on the erythrocyte surface. This micrograph shows both the gamont nucleus (gn) and host cell nucleus (hn). Lateral projections or "flaps" (lf) occur as extensions of the host cell. Micronemes (mn) and the recurved "tail" (rt) are visible. (**B**) Uninfected erythrocyte (e) with a compact nucleus (n) and no alterations of the membrane surface. (**C**) Cross-section of the apical complex, revealing a conoid region (co) with microtubules (mt). A lipid body (lb), microneme bundle (mb), secretory organelles (mn/rh), pellicle (p), and parasitophorous vacuole (pv) are present. (**D**) A projection of host erythrocyte (he) membrane, showing electron dense excrescences (ex) on the membrane surface. (**E**) Mature gamont lying within a host erythrocyte (he), with the recurved "tail" (rt) visible. Structures present are the gamont nucleus (gn), a lateral "flap" (lf) of the host erythrocyte membrane, and secretory organelles (mn/rh). (**F**) Cross-section of the parasite body and recurved "tail" (rt) with a folding region (f). Host erythrocyte (he) shows dehaemoglobinisation and excrescences (ex) on the membrane wall. A microneme (mn) bundle and unknown vesicles (v) were evident in the parasite cytoplasm, as well as a nucleus (gn) with loose chromatin. (**G**) A free gamont, having an elongated shape with narrowing at its centre, which seems to be the reflexed area (ra) when encapsulated within an erythrocyte. The gamont nucleus (gn) is evident at the upper pole, with a shrinkage artefact occurring beside it, on the left. Part of an uninfected erythrocyte (e) occurs at the bottom of the micrograph. (**H**) Micrograph revealing the gamont nucleus (gn), host erythrocyte (he), a retracted host nucleus (hn), lipid bodies (lb), micronemes (mn), microneme bundles (mb), trilaminar pellicle (p), and parasitophorous vacuole (pv). Excrescences occur on the host cell surface, as well as blebbing. (**I**) Micrograph showing detail of the parasite wall. The outer membrane (om) and inner membrane complex (imc) of the pellicle (p) are surrounded by the parasitophorous vacuole (pv). The PV and outer membrane are particularly osmophilic. An excrescence (ex) is evident as a protrusion of the host cell (he) membrane. Micronemes (mn) are present. (**J**) The parasite lying recurved on itself within the host erythrocyte (he), folded nearly completely in half. The gamont nucleus (gn) occurs at the anterior pole and the recurved "tail" (rt) at the posterior pole. The parasite is contained within a pellicle (p) and parasitophorous vacuole (pv).

the parasite appearing elongated, necessitating folding over of the gamont within the host cell.

The erythrocyte cytoplasm showed extensive degenerative changes in haemoglobin content when compared to uninfected erythrocytes. It was also more granulated and irregular in composition, containing rounded cavities that were electron-lucent. In some micrographs, the host nucleus appeared shrunken (Fig. 3H).

The gamont nucleus was large and located centrally, compact with diffuse masses of pale chromatin and no defined nucleolus (Fig. 3H). The margin of the nucleus appeared irregularly osmophilic. Endoplasmic reticulum was not visible on the nucleus periphery, but in some micrographs, the nucleus boundary seems to be undefined, a possible indication that endoplasmic reticulum may occur in these areas (Fig. 3A, E). *Hepatozoon theileri* also had a trilaminar pellicle, with the inner membrane complex bilayered. The outer membrane was highly osmophilic in comparison with the inner membrane complex (Fig. 3I), and also more electron dense than the surrounding parasitophorous vacuole (PV). The PV was depleted of granular contents and withdrawn close to the parasite pellicle so that a compound layer of membranes was visible in many images (Fig. 3E, F, H, J) (Boulard et al. 2001).

SEM of *Hepatozoon theileri*

Surface microscopy presented micrographs showing an elliptical parasite lying along the centre of the host cell, with a clear difference between the surface texture of infected and non-infected erythrocytes (Fig. 4A, B). Erythrocytes parasitised by *H. theileri* were covered by small rounded excrescences on the membrane surface, approximately 7–15 nm in length. These were not arranged according to an ordered pattern, and their shape varied from slightly circular to elongated.

Scanning electron micrographs illustrated the characteristic features of *H. theileri*, such as displacement of the host nucleus (Fig. 4C) and the recurved "tail" of the parasite (Fig. 4D) and the remarkable external changes on the host cell, as well as the external structure of the parasite itself (Fig. 4E). The infected host cell was flattened and ellipsoid, with slightly pointed apices. Two delicate "flaps" protruded from the lateral sides of the parasite. The widest portion of these "flaps" was roughly at the centre of the gamont length but narrowed until the edges of the two opposite "flaps" joined to form the apices on opposite poles (Fig. 4F). These structures were clearly flexible, and easily folded over or gave way when in contact with neighbouring structures (Fig. 4G, H). The lateral "flaps" varied in width, corresponding to the varying length of the long drawn-out erythrocyte projections visible by TEM (Fig. 3A). However, it was found that the flap at the side of the displaced nucleus was often wider than the opposing "flap" (Fig. 4G). The host cell nucleus was visible as a round mass at one end of the parasite, characteristic of nucleus displacement in *H. theileri* as seen by light microscopy. Shrinkage of the host cell nucleus was observed in some infected erythrocytes (Fig. 4E, G).

The surface structure of the parasite itself was visible in one micrograph (Fig. 4E), due to a portion of host cell tissue that was torn away from around the gamont. Its surface texture was observed to be smooth and uniform, besides some wrinkling and folding of the outer parasite tissue.

DISCUSSION

Ultrastructural microscopy revealed that gamonts of both *H. ixoxo* and *H. theileri* have morphological characteristics typical of apicomplexans. Diagnostic features such as the presence of micronemes, rhoptries, a polar ring complex, conoid and a trilaminate pellicle, with the inner membrane bi-laminar, and a parasitophorous vacuole, were observable in both species (Siddall and Desser 1992). Although both parasite species shared the same apicomplexan characters, there were significant morphological differences between the species; certain structures such as the thick capsule with sutures, the polar cap/cavity containing electron dense material of unknown nature, an apicoplast, and an electrophilic nucleolus, all seem to occur only in *H. ixoxo*. Furthermore, *H. theileri* exhibited notable modifications to its host cell that were not observed in cells infected with *H. ixoxo*.

The function and composition of the prominent anterior cap/cavity in *H. ixoxo* is unknown, however, the electron-dense material within this cap may be a waste-product of haemoglobin metabolisms, such as haemosiderin or haemozoin (see Davies and Johnston 2000). However, this proposition requires further biochemical elucidation. The presence of a thick capsule (see Cook et al. 2015; Kvičerová et al. 2014; Široký et al. 2007) and sutures (Boulard et al. 2001; Paperna and Smallridge 2001; Telford 2009) in *H. ixoxo* is alike to those seen characterising the gamonts of species of *Hemolivia*. However, in the case of *Hemolivia* this capsule wall appears impermeable to Giemsa stain and fixation (Boulard et al. 2001; Paperna and Smallridge 2001), with exception to *Hemolivia stellata* (Boulard et al. 2001). Unlike the gamonts of *Hepatozoon* infecting reptiles (Telford 2009), that are rarely encapsulated, encased gamonts have been found in several haemogregarine species that infect African amphibians (see Netherlands et al. 2014a). Thick-walled intraerythrocytic stages with sutures have been found in the snake haemogregarine *Hepatozoon boigae* (Mackerras, 1961), however, these stages were not gamonts, but an unknown parasitic life stage (see Jakes et al. 2003). The sutures of *H. ixoxo* show some similarity to the sutural slits found in the sporocyst walls of the Sarcocystidae, for example, *Toxoplasma gondii* (Nicolle and Manceaux, 1908) (see Speer et al. 1998), *Goussia* species, and *Neospora* species, amongst others (Berto et al. 2014). It was shown by Speer et al. (1998) that the longitudinal suture lines join four sutural plates and facilitate the release of sporozoites from the sporocysts during excystation. This mechanism may provide an indication of the function of suture lines in *H. ixoxo*, and may mechanically aid release of the gamont once blood has been ingested by a haematophagous

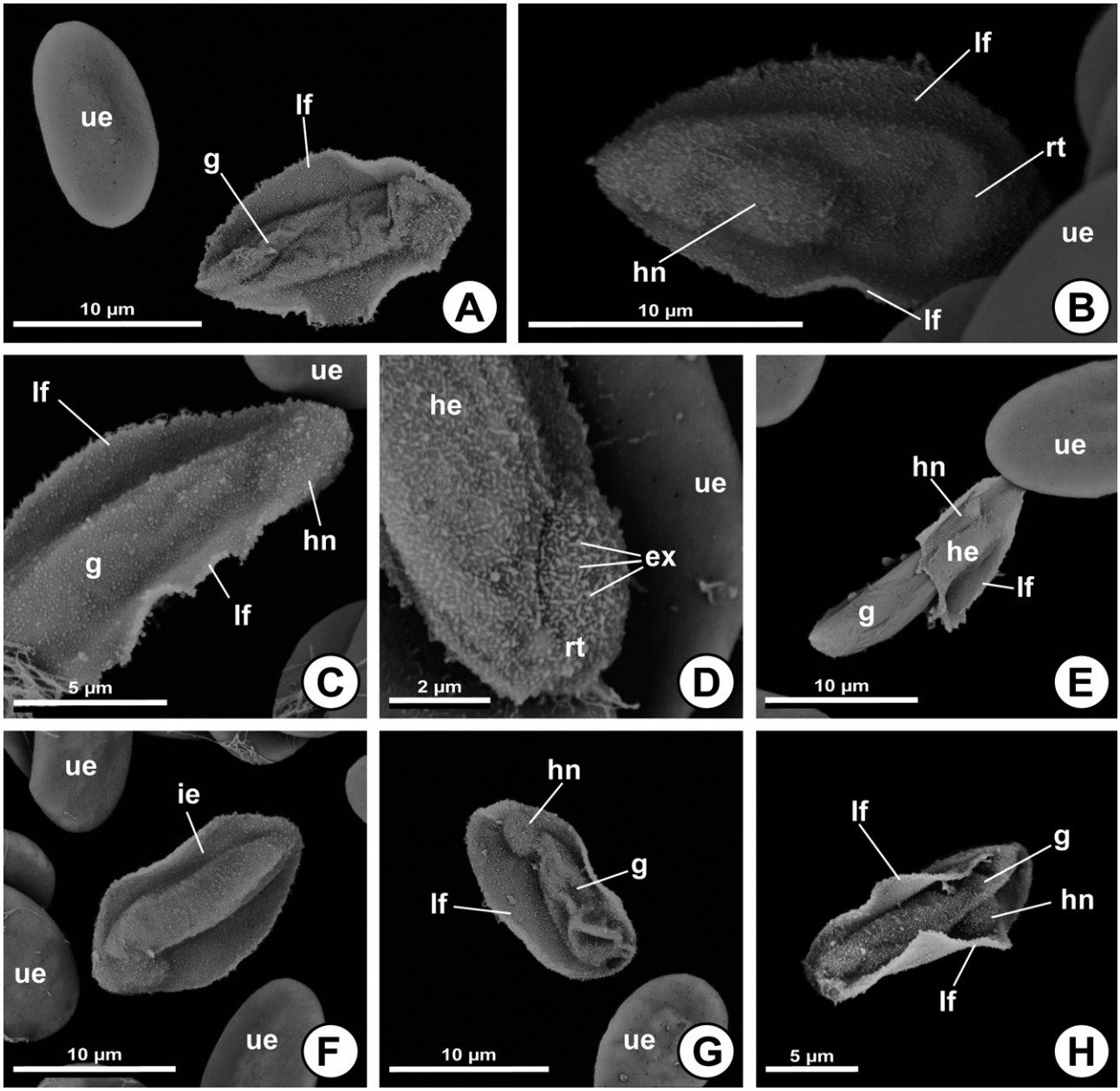

Figure 4 Scanning electron micrographs of *Hepatozoon theileri* in the peripheral blood of *Amietia quecketti*. (**A**) An uninfected (ue) and infected frog erythrocyte. The gamont (g) is visible within the infected erythrocyte and the retraction of cell contents is evident. The cytoskeleton is extended, forming lateral "flaps" (lf). (**B**) Gamont lying within its host cell, showing displacement of the host nucleus (hn) towards the anterior pole, with lateral "flaps" (lf) on both sides adjacent to the gamont, and a recurved "tail" (rt). Uninfected erythrocytes (ue) surround the infected cell. (**C**) Micrograph of the gamont (g) within a host erythrocyte. The displacement of the host nucleus (hn) towards the anterior pole by the presence of the gamont is apparent. Lateral "flaps" (lf) seem flexible and delicate. Uninfected erythrocyte (ue) indicates no changes to external surface structure. (**D**) Detail of the surface structure of an infected (he) and uninfected erythrocyte (ue). The infected erythrocyte surface is extensively scattered with small excrescences (ex). The recurved "tail" (rt) of the gamont appears as a bulge beneath the host erythrocyte (he) membrane. (**E**) Infected erythrocyte (he) with half of its bulk removed, uncovering the residing gamont (g). The gamont surface structure seems relatively smooth with some wrinkling of the tissue. The host nucleus (hn) is extensively retracted. Adjacent to the parasite and host cell lies an uninfected erythrocyte (ue). (**F**) Micrograph at lower magnification showing an infected erythrocyte (i.e.) surrounded by several that are unparasitised (ue). The gamont and host nucleus within the infected erythrocyte are visible. (**G**) Clear view of the frontal plane of the infected erythrocyte showing thinning of the host cell into lateral flaps (lf) adjacent to the gamont (g). The "flap" in which the host nucleus (hn) is situated is wider than the opposite "flap". An uninfected erythrocyte (ue) is visible. (**H**) Micrograph illustrating the flexibility of the lateral "flaps" (lf) adjacent to the residing gamont (g). The host nucleus (hn) is displaced to the one side of the host erythrocyte, and towards the anterior end of the gamont.

arthropod vector. Suture lines found in the of oocyst wall of *Eimeria tenella* (Tyzzer, 1929) were also speculated to enable exystation by Mouafo et al. (2000). It is likely that suture development precedes thick capsule formation, during the early development of intraerythrocytic gamonts (see Paperna and Smallridge 2001).

The plasmalemma of erythrocytes infected with *H. ixoxo* remained neatly intact, which was contrary to the degenerative changes that *H. theileri* was seen to exert on its host cell. The formation of the lateral projections or "flaps" in *H. theileri* is possibly caused by mechanical strain on the cytoskeleton of the erythrocyte as a result of the utilisation of red blood cell haemoglobin and cytoplasm. This may cause the collapse of the membrane onto itself, which might explain why the "flaps" were composed mostly of host cell membrane. For *H. theileri*, TEM revealed blebbing and electron-dense excrescences protruding from the membrane surface of the host cell, which was confirmed by SEM as an external coat of knob-like projections. Similar structures also occur in haemogregarine-infected erythrocytes from other poikilothermic hosts, such as with *Hepatozoon mocassini* (Laveran, 1902) (see Nadler and Miller 1985) and *H. magna* (Paterson et al. 1988) from the amphibian host *Pelophylax kl. esculentus* (formerly *Rana esculenta*) (Desser and Weller 1973). This has also been observed occurring in erythrocytes infected by a species of *Karyolysus* found infecting the lizard *Darevskia raddei* (Boettger, 1892) (syn. *Lacerta saxicola nairensis*) (see Beyer 1977). A serrated appearance with blebbing has also appeared in *H. boigae,* although knob-like structures were not as well-defined (Jakes et al. 2003). The excrescences formed by *H. theileri* resemble those of human erythrocytes infected with *Plasmodium falciparum* (Welch, 1897) (see Aikawa et al. 1983). In the case of *P. falciparum*, excrescences prevent destruction of the parasite by serving as attachment points to endothelial cells of the capillary wall. This prevents transport to the spleen (Davies and Johnston 2000), where the immune system eradicates infected cells. An increase in the adherence of infected red blood cells also causes autoagglutination (aggregation of infected erythrocytes) and rosetting (attachment of uninfected red blood cells to infected ones) (Davies and Johnston 2000). It is possible that autoagglutination aids the parasite in sexual reproduction (facilitating successful initiation of sporogony once gamonts have been ingested by the vector), and rosetting might facilitate reinfection of a clean cell once all resources from its current host cell have been exhausted. Another possible function of membrane alteration may be to change the permeability of the membrane to specific molecules needed by the parasite for metabolism, especially glucose metabolism (Davies and Johnston 2000). Daly et al. (1984) demonstrated through differential staining that an intraerythrocytic *Hepatozoon* species of the snakes *Thamnophis proximus* (Say, 1823) and *Nerodia rhombifera rhombifera* (Hallowell, 1852) altered the plasmalemma of its host cells to increase permeability. The apicomplexan parasite *T. gondii* increases host cell membrane permeability to nucleotides (Pfefferkorn and Pfefferkorn 1977). The permeability of infected erythrocytes is influenced by factors such as the presence of noradrenalin and osmotic swelling (Davies and Johnston 2000).

It is likely that these changes in erythrocyte form and surface structure have some pathological effect on the host. If membrane excrescences formed by *H. theileri* are gamont-derived proteins, an immune response is likely (Davies and Johnston 2000). However, this attack is probably evaded by the alteration of protein gene expression as in *P. falciparum* (see Kilejian et al. 1977). Malformation of the infected erythrocyte shape, possible erythrocyte coagulation and altered blood rheology (see Davies and Johnston 2000), release of cell contents on gamont emergence (Wozniak et al. 1994), and marked haemoglobin depletion may all cause sublethal effects on the host organism (Brown et al. 2006). These effects may be stunted growth, reduced nutritional condition, lower reproductive output, decreased foraging success, and reduced competitive ability among males (Davies and Johnston 2000). It is unclear to what magnitude such sublethal effects caused by *H. theileri* are manifested in the host, *A. quecketti.* In this study and throughout the time, experimental animals were maintained under laboratory conditions, no outward signs of illness or emaciation were observed. However, pathogenicity may be more pronounced when the host is in its natural environment and conditions are more physiologically demanding. In the case of poikilothermic animals, there is little information on pathogenicity of haematozoa on their hosts (Brown et al. 2006; Wozniak et al. 1994), which is contrary to those of birds (Merino et al. 2000) and mammals (see Baneth et al. 2003), which often display sublethal to fatal pathological effects and are therefore more extensively studied. According to Wozniak et al. (1994), haemogregarines are generally well tolerated by their poikilothermic hosts, with parasite-associated mortality being rare. A few studies have shown that haemogregarine species produce no detectable negative impact in their snake hosts, for example, keelback snakes *Tropidonophis mairii* (Gray, 1841), brown tree snakes *Boiga irregularis* (Bechstein, 1802), and slatey-grey snakes *Stegonotus cucullatus* (Duméril, Bibron and Duméril, 1854) (see Brown et al. 2006; Caudell et al. 2002). In contrast, Madsen et al. (2005) found extensive degenerative impacts on life history traits such as growth rate, condition, fecundity, and survival associated with *Hepatozoon* infections and fitness-associated condition factors in the water python *Liasis fuscus* Peters, 1873. Notable pathological effects have also been found in viviparous lizards *Zootoca* (syn. *Lacerta*) *vivipara* (Lichtenstein, 1823) infected with haemogregarines such as the significant reduction in tail regeneration rates as compared to non-parasitised lizards, an increase in the number of immature erythrocytes, reduction in haemoglobin concentration and the total capacity of oxygen fixation (see Oppliger and Clobert 1997; Oppliger et al. 1996).

Different survival strategies of the parasites may explain the morphological diversity exhibited by *H. ixoxo* and *H. theileri*. Gamonts are generally dormant or quiescent developmental stages (Beyer 1977), and it is likely that the dense capsule in *H. ixoxo* enables the parasite to remain for long periods of time in its host cell, as

encasement in haemogregarines is associated with longevity (Paperna and Smallridge 2001). The probability of transmission is increased when the life span of a gamont awaiting ingestion by an arthropod vector is prolonged. Increased longevity of gamonts is a survival strategy for amphibian haemogregarines that corresponds with the physiology of their hosts, as the erythrocyte life spans of ectotherms are generally significantly longer than in endotherms (Davies and Johnston 2000). The polar cap may also increase longevity, if it is a storage organ of the haemoglobin waste-product, as speculated above. A storage organ of this sort would prevent leakage of pigment into the host cell or blood plasma. This function, as well as minimal haemoglobin depletion, would prevent the premature death of the cell and also increase the chance of vector transmission (Paperna and Smallridge 2001). It seems that *H. theileri* exhibits a different life strategy. Instead of preserving the host cell, all resources from the infected erythrocyte are utilised, possibly even nucleus contents, and the gamont moves on to a new host cell once all has been depleted. Haemogregarine gamonts in fresh preparations of recently drawn blood have been observed to easily leave red blood cells, with the ability to remain in the blood plasma for long periods of time, and readily reinfect other cells (Davies and Johnston 2000; Dickson et al. 2013). However, these observations were all performed in vitro and whether or not this is true within the blood stream of the host is not known.

There is a current trend in research to base parasite descriptions on molecular techniques. Fragments of the 18S rRNA gene have been widely used to characterise species and infer phylogenetic relationships among apicomplexans (Barta et al. 2012), although ITS-1 DNA and mitochondrial DNA have also been used (Boulianne et al. 2007; Kim et al. 1998; Leveille et al. 2014). Our results and also previous studies (Netherlands et al. 2014a,b) show that both *H. theileri* and *H. ixoxo* are closely related based on fragments of the 18S rRNA gene. Although molecular work may be an effective tool in differentiating between parasite species, it still remains but one component in the descriptive process of a haemogregarine parasite. The morphological description of a haemogregarine may be time-consuming but is still necessary. Recently, morphological descriptions have included only features as seen by light microscopy, however, this study has highlighted that further morphological differences may be seen at an ultrastructural level. It was apparent using light microscopy that both *H. ixoxo* and *H. theileri* cause hypertrophy of the host cell (Netherlands et al. 2014a,b). Although the TEM results confirmed hypertrophy of cells infected with *H. ixoxo,* electron microscopy revealed that the apparent "hypertrophy" seen in erythrocytes infected with *H. theileri* is not due to hypertrophy, but due to the lateral "flaps" caused by distension and flattening of the cell outline. Unfortunately, use of these methods has been declining, regardless of the suggestions of their importance made almost two decades ago. Furthermore, ultrastructural studies are not only useful for increasing the robustness of species comparisons and phylogenetic placement but may also indicate relationships between host pathology and parasite-induced modifications of the host cell. It was suggested by Smith et al. (1999) that these pathological effects may be an additional source of information in species characterisation. Parasite-induced membrane alterations have been found in few other haemogregarine species, not because the phenomenon is rare, but due to the lack of ultrastructural studies performed on these organisms. This study recommends that further studies be performed on parasite morphology and the resulting pathogenicity of host cell alterations. It is also possible that the differences in morphology are somehow related to the behaviour and ecology of the vector, but further elucidation of the life cycles of these haemogregarines is necessary before inferences can be made.

ACKNOWLEDGMENTS

We are grateful towards the North-West University Botanical Gardens, the Ndumo Game Reserve, and the Kwa Nyamazane Conservancy for permission to collect samples and do fieldwork, and the African Amphibian Conservation Research Group for help in collecting specimens. The school of Microbiology, Unit for Environmental Sciences and Management (NWU-PC), are thanked for the use of their facilities for molecular work. Ezemvelo KZN Wildlife is thanked for research permits OP 674/2012, OP 5139/2012, OP 526/2014, and OP 839/2014. Some of the fieldwork and running expenses of this work was funded by the Water Research Commission (WRC) of South Africa (Project K5-2185, NJ Smit, PI).

LITERATURE CITED

Aikawa, M., Rabbege, J. R., Udeinya, I. & Miller, E. H. 1983. Electron microscopy of knobs in *Plasmodium falciparum* infected erythrocytes. *J. Parasitol.*, 69:435–437.

Baneth, G., Mathew, J. S., Shkap, V., Macintire, D. K., Barta, J. R. & Ewing, S. A. 2003. Canine hepatozoonosis: two disease syndromes caused by separate *Hepatozoon* spp. *Trends Parasitol.*, 19:27–31.

Barta, J. R., Ogedengbe, J. D., Martin, D. S. & Smith, T. G. 2012. Phylogenetic position of the adeleorinid coccidia (Myzozoa, Apicomplexa, Coccidia, Eucoccidiorida, Adeleorina) inferred using 18S rDNA sequences. *J. Eukaryot. Microbiol.*, 59:171–180.

Berto, B. P., McIntosh, D. & Lopes, C. W. G. 2014. Studies on coccidian oocysts (Apicomplexa: Eucoccidiorida). *Rev. Bras. Parasitol. Vet.*, 23:1–15.

Beyer, T. 1977. Electron microscope study of *Karyolysus* sp. (Sporozoa: Adeleida: Haemogregarinidae) and of changes induced in the infected host cell. *Protistologica*, 13:57–66.

Boulard, Y., Paperna, I., Petit, G. & Landau, I. 2001. Ultrastructure of developmental stages of *Hemolivia stellata* (Apicomplexa: Haemogregarinidae) in the cane toad *Bufo marinus* and in its vector tick *Amblyomma rotondatum*. *Parasitol. Res.*, 87:589–604.

Boulianne, B., Evans, R. C. & Smith, T. G. 2007. Phylogenetic analysis of *Hepatozoon* species (Apicomplexa: Adeleorina) infecting frogs of Nova Scotia, Canada, determined by ITS-1 sequences. *J. Parasitol.*, 93:1435–1441.

Brown, G. P., Shilton, C. M. & Shine, R. 2006. Do parasites matter? Assessing the fitness consequences of haemogregarine infection in snakes. *Can. J. Zool.*, 84:668–676.

Caudell, J. N., Whittier, J. & Conover, M. R. 2002. The effects of haemogregarine-like parasites on brown tree snakes (*Boiga irregularis*) and slatey-grey snakes (*Stegonotus cucullatus*) in Queensland, Australia. *Int. Biodeter. Biodegr.*, 49:113–119.

Cook, C. A., Netherlands, E. C. & Smit, N. J. 2015. First *Hemolivia* from southern Africa: reassigning chelonian *Haemogregarina parvula* Dias, 1953 (Adeleorina: Haemogregarinidae) to *Hemolivia* (Adeleorina: Karyolysidae). *Afr. Zool.*, 50:165–173.

Daly, J. J., McDaniel, R. C., Townsend, J. W. & Calhoun Jr, C. H. 1984. Alterations in the plasma membranes of *Hepatozoon*-infected snake erythrocytes as evidenced by differential staining. *J. Parasitol.*, 70:151–153.

Davies, A. J. & Johnston, M. R. L. 2000. The biology of some intraerythrocytic parasites of fishes, amphibia and reptiles. *Adv. Parasitol.*, 45:1–107.

Desser, S. S. & Weller, I. 1973. Structure, cytochemistry and locomotion of *Haemogregarina* sp. from *Rana berlandieri*. *J. Protozool.*, 20:65–73.

Dickson, C. M., Ogbuah, C. T. & Smith, T. G. 2013. The role of gamont entry into erythrocytes in the specificity of *Hepatozoon* species (Apicomplexa: Adeleida) for their frog hosts. *J. Parasitol.*, 99:1028–1033.

Jakes, K. A., O'Donoghue, P. J. & Whittier, J. 2003. Ultrastructure of *Hepatozoon boigae* (Mackerras, 1961) nov. comb. from brown tree snakes, *Boiga irregularis*, from northern Australia. *Parasitol. Res.*, 90:225–231.

Kilejian, A., Abati, A. & Trager, W. 1977. *Plasmodium falciparum* and *Plasmodium coatneyi*: immunogenicity of "knob-like protrusions" on infected erythrocyte membranes. *Exp. Parasitol.*, 42:157–164.

Kim, B., Smith, T. G. & Desser, S. S. 1998. The life history and host specificity of *Hepatozoon clamatae* (Apicomplexa: Adeleorina) and ITS-1 nucleotide sequence variation of *Hepatozoon* species of frogs and mosquitoes from Ontario. *J. Parasitol.*, 84:789–797.

Kvičerová, J., Hypša, V., Dvořáková, N., Mikulíček, P., Jandzik, D., Gardner, G. M., Javanbakht, H., Tiar, G. & Široký, P. 2014. *Hemolivia* and *Hepatozoon*: haemogregarines with tangled evolutionary relationships. *Protist*, 165:688–700.

Leveille, A. N., Ogedengbe, M. E., Hafeez, M. A., Tu, H. & Barta, J. R. 2014. The complete mitochondrial genome sequence of *Hepatozoon catesbianae* (Apicomplexa: Coccidia: Adeleorina), a blood parasite of the Green frog, *Lithobates* (formerly *Rana*) *clamitans*. *J. Parasitol.*, 100:651–656.

Madsen, T., Ujvari, B. & Olsson, M. 2005. Old pythons stay fit; effects of haematozoan infections on life history traits of a large tropical predator. *Oecologia*, 142:407–412.

Merino, S., Moreno, J., Sanz, J. J. & Arriero, E. 2000. Are avian blood parasites pathogenic in the wild? A medication experiment in blue tits (*Parus caeruleus*). *Proc. Roy. Soc. Lond. B: Biol. Sci.*, 267:2507–2510.

Mouafo, A. N., Richard, F. & Entzeroth, R. 2000. Observation of sutures in the oocyst wall of Eimeria tenella (Apicomplexa). *Parasitol. Res.*, 86:1015–1017.

Nadler, S. A. & Miller, J. H. 1985. Fine structure of *Hepatozoon mocassini* (Apicomplexa: Eucoccidiorida) gamonts and modifications of infected erythrocyte plasmalemma. *J. Protozool.*, 32:275–279.

Netherlands, E. C., Cook, C. A., du Kruger, D. J. D., Preez, L. H. & Smit, N. J. 2015. Biodiversity of frog haemoparasites from sub-tropical northern KwaZulu-Natal, South Africa. *Int. J. Parasitol. Parasites Wildl.*, 4:135–141.

Netherlands, E. C., Cook, C. A. & Smit, N. J. 2014a. *Hepatozoon* species (Adeleorina: Hepatozoidae) of African bufonids, with morphological description and molecular diagnosis of *Hepatozoon ixoxo* sp. nov. parasitising three *Amietophrynus* species (Anura: Bufonidae). *Parasit. Vectors*, 7:552.

Netherlands, E. C., Cook, C. A., Smit, N. J. & du Preez, L. H. 2014b. Redescription and molecular diagnosis of *Hepatozoon theileri* (Laveran, 1905) (Apicomplexa: Adeleorina: Hepatozoidae), infecting *Amietia quecketti* (Anura: Pyxicephalidae). *Folia Parasitol.*, 61:239–300.

Oppliger, A., Célérier, M. L. & Clobert, J. 1996. Physiological and behavioral changes in the common lizard parasitized by haemogregarines. *Parasitology*, 113:433–438.

Oppliger, A. & Clobert, J. 1997. Reduced tail regeneration in the common lizard, *Lacerta vivipara*, parasitized by blood parasites. *Funct. Ecol.*, 11:652–655.

Ostrovska, K. & Paperna, I. 1990. *Cryptosporidium* sp. of the starred lizard *Agama stellio*: ultrastructure and life cycle. *Parasitol. Res.*, 76:712–720.

Paperna, I. & Smallridge, C. J. 2001. Ultrastructure of developmental stages of *Hemolivia mariae* (Apicomplexa: Haemogregarinidae), natural parasite of the Australian sleepy lizard, in experimentally infected deviant hosts. *Folia Parasitol.*, 48:255–262.

Paterson, W. B., Desser, S. S. & Barta, J. R. 1988. Ultrastructural features of the apical complex, pellicle and membranes investing the gamonts of *Haemogregarina magna* (Apicomplexa: Adeleina). *J. Protozool.*, 35:73–80.

Pfefferkorn, E. R. & Pfefferkorn, L. C. 1977. *Toxoplasma gondii*: specific labelling of nucleic acids of intracellular parasites in Lesch-Nyhan cells. *Exp. Parasitol.*, 41:95–104.

Siddall, M. E. & Desser, S. S. 1992. Ultrastructure of gametogenesis and sporogony of *Haemogregarina* (sensu lato) *myoxocephali* (Apicomplexa: Adeleina) in the marine leech *Malmiana scorpii*. *J. Protozool.*, 39:545–554.

Široký, P., Kamler, M., Frye, F. L., Fictum, P. & Modrý, D. 2007. Endogenous development of *Hemolivia mauritanica* (Apicomplexa: Adeleina: Haemogregarinidae) in the marginated tortoise *Testudo marginata* (Reptilia: Testudinidae): evidence from experimental infection. *Folia Parasitol.*, 54:13–18.

Smith, T. G. 1996. The genus *Hepatozoon* (Apicomplexa: Adeleina). *J. Parasitol.*, 82:565–585.

Smith, T. G. & Desser, S. S. 1997. Ultrastructural features of the gametogenic and sporogonic development of *Hepatozoon sipedon* (Apicomplexa: Adeleorina): the applicability of ultrastructural data in differentiating among *Hepatozoon* species. *Parasite*, 4:141–151.

Smith, T. G., Kim, B. & Desser, S. S. 1999. Phylogenetic relationships among *Hepatozoon* species from snakes, frogs, and mosquitoes of Ontario, Canada, determined by ITS-1 nucleotide sequences and life-cycle, morphological and developmental characteristics. *Int. J. Parasitol.*, 29:293–304.

Speer, C. A., Clark, S. & Dubey, J. P. 1998. Ultrastructure of the oocysts, sporocysts, and sporozoites of *Toxoplasma gondii*. *J. Parasitol.*, 84:504–512.

Telford, S. R. 2009. Hemoparasites of the reptilia: Color atlas and text. CRC Press, New York. p. 199–259.

Todd, W. J. 1986. Effects of specimen preparation on the apparent ultrastructure of microorganisms. *In:* Aldrich, H. C. & Todd, W. J. (ed.), Ultrastructure Techniques for Microorganisms. Plenum Press, New York. p. 87–100.

Wozniak, E. J., McLaughlin, G. L. & Telford Jr, S. R. 1994. Description of the vertebrate stages of a hemogregarine species naturally infecting Mojave Desert sidewinders (*Crotalus cerastes cerastes*). *J. Zoo Wildl. Med.*, 25:103–110.